The Basel tracking algorithm in the DIRAC experiment.

Christian P. Schütz* Ludwig Tauscher

University of Basel

June 2003

Abstract

This note describes the Basel tracking algorithm in the DIRAC experiment. It makes use of the drift chamber information downstream to define a track. This track is then extrapolated to the upstream detectors where the total momentum is adjusted with a hit SFD fiber. A Kalman filter algorithm extrapolates the track further up to the target, where the absolute and relative momenta are calculated.

1 Introduction

The BASEL extended tracking for the DIRAC experiment[1] is a development based on the standard offline code ARIANE [2]. It was developed to improve on some issues of the standard tracking procedure and has therefore also influenced the standard ARIANE tracking code. By virtue of its independence it can also be used to cross-check results obtained from the standard DIRAC tracking code.

The tracking procedure for pion pairs in the DIRAC experiment can be separated into two parts: downstream and upstream tracking. In addition, the tracking algorithm itself can be split into pattern recognition (i.e. track finding) and track fitting.

The tracking algorithm starts at the downstream detectors. Each track is measured with high precision in the drift chambers. The relative timing of the two tracks is obtained from the time-of-flight information of the vertical hodoscopes.

*Corresponding author: Christian Schütz, CERN, 585-R-005, CH-1211 Geneva 23, phone +41 22 767 38 91, email christian.schuetz@cern.ch.

The absolute total lab momentum p_{tot} is determined by the drift chamber information, by the parametrized magnetic field and the position of the target, which is assumed to be the origin of the particles. The total momentum is then fine-adjusted with the X plane of the SFD detector. Making use of a Kalman filter and the target as a supplementary measurement point, one finds the x and y projections of the total momentum. The ionisation hodoscopes (IH) are used to resolve ambiguities between hit SFD columns. Once the total momentum is found, the relative momentum Q can be determined. Since the two pions have small relative opening angle, Q in the center of mass system (CMS) is also small.

This note is organised as follows: First a quick overview of the Kalman filter procedure is given. Then the Basel track finding and track fitting is explained. Finally the Λ decay is used to demonstrate the precision of the absolute momentum determination. The resolution of the tracking is established using Monte Carlo data.

2 Kalman Filter

The Kalman filter algorithm has a 'progressive' approach. It first predicts for each measurement an extrapolated state at this point, then it corrects it with the measurement to yield the final filtered value. The filtered value is the best estimate of the state, taking into account all prior measurements.

This is exactly the progressive approach of the filter: It updates the state and its covariance matrix with every measurement. Hence the predictions become more and more accurate.

2.1 Prediction

For each measurement point, the algorithm first calculates a prediction. This prediction is based on the '**System Equation**', which describes the evolution of the true state of our system, i.e.

$$x_{t+1} = A_t x_t + \omega_t \tag{1}$$

Here x_{t+1} and x_t denote the state at times t+1 and t, A_t is a (n$\times$n)matrix, that incorporates the evolution of the system from time t to time t+1. ω_t represents the white, Gaussian-distributed noise of the process. Its mean equals 0. Whiteness implies that the process noise is not correlated in time.

For tracking purposes, the state vector x_t incorporates the coordinates and the

velocity vector of the particle at any given time t, i. e.

$$x = \begin{pmatrix} Coordinate\ 1 \\ Coordinate\ 2 \\ \cdots \\ Velocity\ 1 \\ Velocity\ 2 \\ \cdots \end{pmatrix}$$

The evolution matrix A describes how the coordinates and the velocities change over time. This can be a straight line for the case of no external field, but it can also be a circle or a helix for example, if there is a magnetic field present. The process noise ω_t is the multiple scattering at time t. It changes the state vector randomly.

If, for example, we have a two-dimensional space (yz) with no external field and a particle moving with constant speed (no energy loss) along the z-axis, the system equation can be written as (see Eq.1):

$$x = \begin{pmatrix} y \\ v_y \end{pmatrix} \xrightarrow{(1)} \begin{pmatrix} y_{t+1} \\ v_{y_{t+1}} \end{pmatrix} = \begin{pmatrix} 1 & \Delta t \\ 0 & 1 \end{pmatrix} \cdot \begin{pmatrix} y_t \\ v_{y_t} \end{pmatrix} + \begin{pmatrix} \delta y_t \\ \delta v_{y_t} \end{pmatrix} \tag{2}$$

The y coordinate at any time t+1 can be written as

$$y_{t+1} = y_t + v_{y_t} \cdot \Delta t + \delta y_t \tag{3}$$

The multiple scattering (MS) δy_t changes the y coordinates randomly. The velocity vector v_{y_t} is also changed by the MS process at each scatterer:

$$v_{y_{t+1}} = v_{y_t} + \delta v_{y_t}$$

So y_{t+1} and $v_{y_{t+1}}$ have to be updated after each scatterer.

The true state x_t is not known, but one can give an estimate $\hat{x}_t$. To predict the state at time t+1 the best we can do is (since we don't know the true MS, we set it equal to its mean, which is zero):

$$E[x_{t+1}] = \hat{x}^P_{t+1} = A\hat{x}_t \tag{4}$$

The index P denotes prediction. Not only can we predict the state at time t+1, also the covariance matrix $P_{\hat{x}_t}$ of the state at time t can be extrapolated to t+1:

$$E[(x_{t+1} - \hat{x}^P_{t+1})(x_{t+1} - \hat{x}^P_{t+1})^T] = P^P_{\hat{x}_{t+1}} = AP_{\hat{x}_t}A^T + \Omega \tag{5}$$

Ω is the covariance matrix of the process noise ω and is connected in the following way:

$$p(\omega) \sim N(0, \Omega)$$

where N(...) represents a normal probability distribution.

2.2 Correction

If we obtain a measurement z_{t+1} at time t+1, we can 'correct' the prediction of the state with this measurement. The measurement itself has an error r_{t+1} and is connected to the true state by the '**Measurement Equation**':

$$z_{t+1} = H \cdot x_{t+1} + r_{t+1} \tag{6}$$

The linear (m×n) matrix H translates the true state x_t to the frame of the measurement z_t. r_t represents the measurement error which is also white and Gaussian-distributed around 0. It is connected to the measurement noise covariance matrix R_t by:

$$p(r) \sim N(0, R)$$

where N(...) represents a normal probability distribution.

For our example above, if we have a detector measuring the y coordinate, equation (6) becomes:

$$z_{t+1} = \begin{pmatrix} 1 & 0 \end{pmatrix} \cdot \begin{pmatrix} y_{t+1} \\ v_{y_{t+1}} \end{pmatrix} + r_{t+1} \tag{7}$$

$$z_{t+1} = y_{t+1} + r_{t+1}$$

This makes sense: The measured y value is composed of the y coordinate of the true state plus the measurement error.
The weights of how the prediction and the measurement enter into the corrected (=filtered) value are incorporated in the **gain matrix K**:

$$K_{t+1} := \frac{P^P_{\hat{x}_{t+1}} H^T}{R_{t+1} + H P^P_{\hat{x}_{t+1}} H^T} \tag{8}$$

Now we can correct the predicted value and its covariance matrix by applying the weights in K:

$$\hat{x}^F_{t+1} = \hat{x}^P_{t+1} + K_{t+1}\{z_{t+1} - H\hat{x}^P_{t+1}\} \tag{9}$$

F stands for 'filtered' (= corrected). The filtered covariance matrix becomes:

$$P^F_{\hat{x}_{t+1}} = \{I - K_{t+1}H\}P^P_{\hat{x}_{t+1}} \tag{10}$$

What does this imply ? The gain matrix K weights the measurement and the prediction of a state at time t+1 according to their relative errors. This can easily be seen by taking the limit of no measurement error

$$\lim_{R_{t+1}\to 0} K = H^{-1} \xrightarrow{(9)} \hat{x}^F_{t+1} = H^{-1} z_{t+1} = \hat{x}_{t+1} \tag{11}$$

In this case $\hat{x}^F_{t+1}$ becomes simply $H^{-1}z_{t+1} = \hat{x}_{t+1}$. The more accurate the measurement is compared to the prediction, the more it is weighted. In the limit of no measurement error, only the measurement is used. The same logic applies vice versa. For no prediction error

$$\lim_{P^P_{\hat{x}_{t+1}} \to 0} K = 0 \xrightarrow{(9)} \hat{x}^F_{t+1} = \hat{x}^P_{t+1} \tag{12}$$

K becomes zero and $\hat{x}^F_{t+1}$ is equal to $\hat{x}^P_{t+1}$. The measurement has no influence on the filtered value for this case.

Prediction - Correction View Therefore the Kalman Filter algorithm can be seen as a feedback control. It predicts the state at some time and then corrects it by some (noisy) measurement.

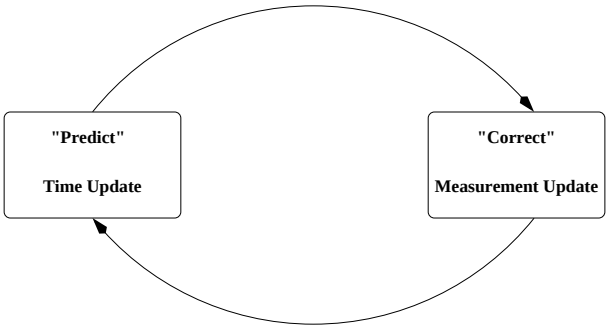

Figure 1: The ongoing Kalman Filter cycle. Time Update predicts the current state estimate ahead in time. The measurement update corrects the projected estimate by an actual measurement at that time.

2.3 Error of Prediction

The mean $\hat{x}^F_t$ and the covariance matrix $P^F_{\hat{x}_t}$ fully describe the Gaussian-distributed conditional probability density function of the true state x_t. But what would be interesting in this context is the distribution of the error of the estimate, denoted as

$$e_t = x_t - \hat{x}^F_t \tag{13}$$

It can be shown that (Maybeck[3], P.226)

$$E[e_t | z_t, z_{t-1}, ...] = 0 \tag{14}$$

and

$$E[e_t e_t^T | z_t, z_{t-1}, ...] = P^F_{\hat{x}_t} \tag{15}$$

Thus, $\hat{x}^F_t$ is an unbiased estimate of the true state. In addition, the $P^F_{\hat{x}_t}$ calculated through (10) assumes additional significance: it is the covariance to describe the Gaussian error committed to the estimate.

2.4 Optimality Criterion

As already stated, $\hat{x}^F_t$ is the optimal estimate of the true state x_t given all prior measurements. It is optimal in the sense, that it is the mean, the median and the maximum likelihood estimate of the entire probability density function of x_t, conditioned on all available information (prior measurements). The covariance $P^F_{\hat{x}_t}$ can then be seen as either the covariance of this conditioned probability density function, as well as the covariance of the Gaussian error between x_t and $\hat{x}^F_t$.

Another optimality criterion for an estimate $\hat{x}^F_t$ would be, that it minimises the covariance

$$E[ee^T], \qquad \text{where} \qquad e_t = x_t - \hat{x}^F_t. \qquad \text{(see equation 13)}$$

It is then called the minimum mean square error estimate (MMSE). By virtue of being the conditional mean, $\hat{x}^F_t$ is also the MMSE.

In fact it can be shown, that the conditional mean of a Gaussian-distributed cond.p.d.f. minimises any function of the form $E[eMe^T]$. As a consequence, also the least square sum over all filtered residuals $[z_t - H\hat{x}^F_t]$ with any weight matrix M is minimised:

$$\chi^2 = \sum_{t=1}^{n} [z_t - H\hat{x}^F_t]\, M\, [z_t - H\hat{x}^F_t]^T \tag{16}$$

Specifically, one can choose the covariance matrix Q^F_t of the filtered residuals: $M = (Q^F_t)^{-1} = (R_t - H_t P^F_t H^T_t)^{-1}$. For Q^F_t to have an inverse matrix, it has to be positive definite.

This means for our previous example that the χ^2 sum of the residuals

$$[z_t - H\hat{x}^F_t] = z_t - z^F_t \tag{17}$$

is minimised. $(z_t)^F$ is the transformation of the filtered value in the z-measurement frame.

3 Downstream track finding and fitting

The BASEL tracking algorithm starts downstream by fitting a straight line using the information available from the drift chambers, the vertical hodoscopes (VH) and the horizontal hodoscopes (HH) and the preshower (PrSh). Once a track is established, a first approximation to the total lab momentum can be calculated.

3.1 Selection of track candidates

As a first step the drift chamber information is used to construct tracks by hit wires and drift times. The algorithm forms a 'track road' connecting the hits from the wires in the first and the last plane of x (or y) orientation to a straight line. The intrapolated intersections of this straight line with the other DC planes are then compared to the measured hits. If there are more than three measured hits close to the constructed line on all DC planes together, the constructed line becomes a track candidate.

Once a track candidate is established, the tracking program extrapolates it to the VH and the HH detectors and checks whether it matches a hit slab geometrically and timewise. In addition, a correlated hit is also required in the PrSh. All track candidates with corresponding hits are selected for further processing.

The number of found track candidates depends mostly on the efficiency of the DC reconstruction which in turn is related to the intensity of the incoming beam. For the whole of 2001 we have around 96% with only one track candidate for the negative arm, and 92% for the positive one[1]. The remaining events are predominantely two-track events.

Due to the increased ambiguity which events with higher track multiplicities generate at the SFD, we reject higher multiplicity events.

3.2 Track fitting

The next stage of the tracking algorithm establishes the parameters of the track candidates found in the DC's using a χ^2 fit[2]. In general terms, the track parameters θ are the solution to the equation

$$\begin{pmatrix} a_{11} & \cdots & a_{1n} \\ \vdots & \ddots & \vdots \\ a_{n1} & \cdots & a_{nn} \end{pmatrix} \begin{pmatrix} \theta_1 \\ \vdots \\ \theta_n \end{pmatrix} = \begin{pmatrix} m_1 \\ \vdots \\ m_n \end{pmatrix} \tag{18}$$

[1]The difference between the positive and the negative arm stems mostly from additional proton admixture in the positive arm and the trigger, which starts with a signal in the positive arm.

[2]This stage is identical to ARIANE. A very detailed description of the DC track fit can be found here [4]. What follows is a short explanation of the used procedure.

The vector m contains the measured coordinate in the local frame[3]. The matrix A is a transformation matrix. The length of the measurement vector m is up to $L_m = 14$. Assuming a straight line, the track is described by 6 parameters: 3 coordinates and 3 angles (θ_X, θ_Y,θ_Z, θ_{ax}, θ_{ay}, θ_{az}).

To reduce the parameter space, we define for all track candidates the parameter θ_Z as the Z-coordinate of the exit membrane of the vacuum chamber in front of the DC planes. In addition, the angles are defined with respect to θ_{az}, so that we can set $\theta_{az} = 1$. This reduces the number of parameters to 4 and the dimensions of the transformation matrix A to $[L_m, 4]$. The measurement errors which are induced by multiple scattering define the measurement error matrix D. Its component D_{ij} for example corresponds to the uncertainty induced by the multiple scattering in plane i on the measurement in plane j.

If we now apply the standard χ^2 method, defining the error matrix of the track parameters as E_θ, we obtain:

$$B = A^T \cdot D^{-1} \cdot A$$
$$\theta = B^{-1} \cdot A^T \cdot D^{-1} \cdot m$$

The errors of the track parameters can be calculated as:

$$E_\theta = B^{-1}$$

and the χ^2 value is equal to:

$$\chi^2 = (m - A \cdot \theta)^T \cdot D^{-1} \cdot (m - A \cdot \theta)$$

3.3 Momentum determination I

Once the DC track parameters are established, one can generate a first momentum determination which relies on the assumption, that the track originates from the target. This is possible, because there exists a unique relation, see equation 19, assuming a homogeneous magnetic field in y direction, with no magnetic field component in x and z direction (Fernow [5], P. 327):

$$\sin(a) + \sin(b) = \frac{\int B\, dl}{3.33p} \tag{19}$$

Where a and b are the incident and exit angle, B is the magnetic field in y direction, p the total momentum of the particle and dl is the integration over the path of the particle in the magnetic field, see figure 2.

[3]The local frame has only one coordinate. It is the matrix A which transformes the track parameters from the global to the local frame.

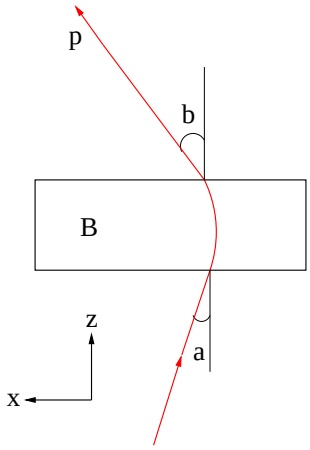

Figure 2: Scheme of the particle flying through the magnet. a is the entrance angle, b the exit angle, B the vertical magnetic field in y direction and p is the absolute value of the total momentum.

The calculation itself is done by an iterative procedure. The magnetic field is described in polynomial form. The momentum determination and the track parameters obtained with the DC fit allow to extrapolate the DC track to the upstream detectors. In addition, the tracks need to be within the geometrical magent aperture as well as within the active area of the upstream detectors.

4 Upstream track finding and fitting

The upstream track finding and fitting first refines the total momentum determination using a measurement in the SFD X plane. It then uses a Kalman filter to lead the track through the other SFD plane to the target.

4.1 Ambiguity of prompt events

The signal events we are looking for exhibit very small time differences. The accidental pairs on the other hand have well defined absolute time differences of more than 5 ns. This leads to a different treatment of prompt versus accidental events.

If the tracks of a prompt event are extrapolated to the upstream detectors, there are mostly two good hit candidates for each track to choose from. For accidental pairs, due to their large time difference, there is normally just one.

Figure 3 illustrates the problem: For prompt events, $|t_3 - t_4| < 0.5ns \rightarrow |t_1 - t_2| < 4.2$ ns (at 3σ confidence level). The chosen time cut for the SFD X

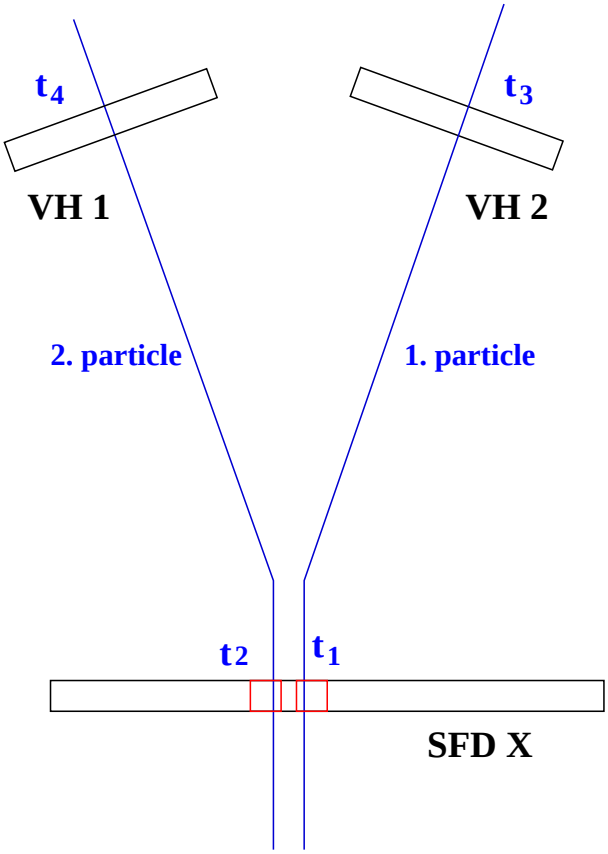

Figure 3: Measured times upstream and downstream in the DIRAC setup for $\pi^+\pi^-$ pairs.

plane (details see below) would accept both hits for both particles. For a typical accidental event, however, the time difference at the level of VH is around 10 ns. This leads to an equal time difference at the level of SFD X. Due to the time cut, the tracking would thus only find one good hit candidate per track.

In order to treat prompt and accidental events equal, we search for hit candidates in the upstream detectors using the time information of both arms: Track 1 is extrapolated to SFD X using its intrinsic time in the VH, t_3, but also the VH time of the other track, t_4. Thus each track has two time information per SFD plane. Such a mechanism makes sure that both, prompt and accidental pair events, are treated equally.

This method is applied to find hit candidates on both layers of the SFD.

4.2 Track finding in SFD X

In a first step the measurements of the X plane in the SFD detector are checked against a geometrical (equation 20) and time cut (equation 21).

Geometrical cut For the geometrical cut we use as ARIANE a 3 σ interval taking into account the multiple scattering. The beam movement is also considered by adding 0.2cm. This defines a total acceptance region for hit candidates on the SFD X layer of:

$$\text{Acceptance region} = 0.2 + \frac{4.8}{p_{tot}} \text{ cm} \tag{20}$$

Time cut For the time cut we use a slightly looser cut. In agreement with ARIANE we accept measurements that occur within 4 ns around the predicted time of the track:

$$\Delta t \text{ (VH} \rightarrow \text{SFD X)} \leq \text{ Time of Flight } \pm 4 \text{ ns} \tag{21}$$

Judging from figure 4, this amounts to more than 3σ acceptance.

The measurement closest to the extrapolation is consequently selected for each track.

Double ionisation cut In case both tracks select the same hit fiber on SFD X, the tracking algorithm checks the ionisation hodoscopes. Specifically it looks in the first two X layers of the DeDx detector for a time- and space correlated hit pattern originating from a double ionisation hit or from two adjaciant single ionisation hits. If there is such a pattern, the event is accepted. If not, the program looks for a close-lying second hit around in the SFD X to move one of the tracks to this second hit. Which track is moved to the other hit candidate is decided at random. The resulting decision tree is shown graphically in figure 5.

4.3 Momentum refinement using the SFD X hits

Once the hit SFD X fibers is established, the total laboratory momentum of the track is fine-adjusted. This fine-tuning is an iterative procedure: The total momentum of the track is adjusted so that it passes exactly through the selected hit fiber. This is achieved by Taylor expanding the function (the θ vector incorporates the track parameters):

$$\theta_{upstream} = f(\theta_{DC}, p_{tot}) \tag{22}$$

up to the linear term with respect to the total momentum p_{tot}:

$$p_{tot}^1 = p_{tot}^0 + \frac{dp_{tot}}{dx} \cdot dx^0 \tag{23}$$

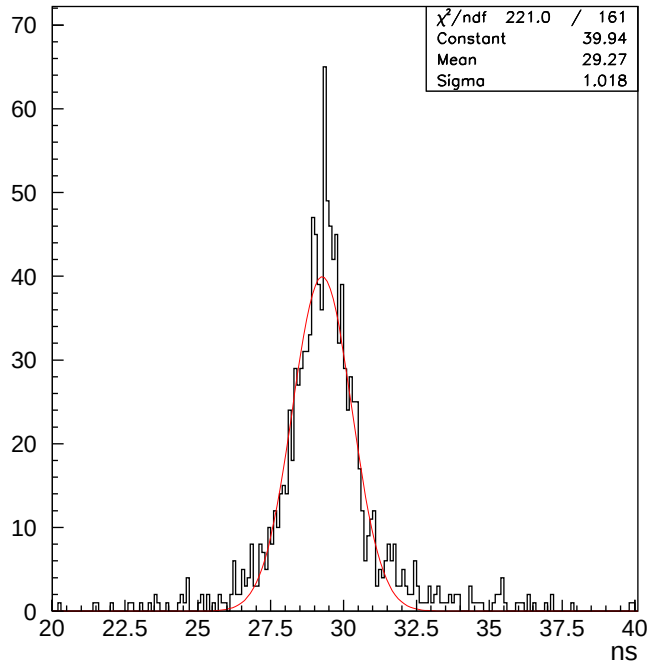

Figure 4: Time difference for single tracks between VH and SFD X. All events are required to have only one hit per SFD plane. The $\sigma_t \approx 1ns$, so a 3 σ environment would correspond to 3 ns.

p^0_{tot} is the zero-th approximation of the momentum (see section 3.3). p^1_{tot} becomes the linear correction of the total momentum. dx^0 is the difference between the estimated x coordinate of the track, x^0_{track}, using p^0_{tot}, and the desired hit fiber:

$$dx^0 = x^0_{track} - x_{fiber} \tag{24}$$

The iteration algorithm now uses p^1_{tot} to obtain x^1_{track} and dx^1. Then the second correction to the total momentum is calculated:

$$dx^1 = x^1_{track} - x_{fiber}$$

$$p^2_{tot} = p^1_{tot} + \frac{dp_{tot}}{dx} \cdot dx^1$$

P_{tot} is refined until dx becomes small as compared to the SFD fiber width (10^{-3}).

4.4 Smearing P_x within one fiber

The tracking algorithm also allows to distribute the track over the entire fiber width in order to smear P_x. For this purpose, x_{fiber} is uniformly chosen over the

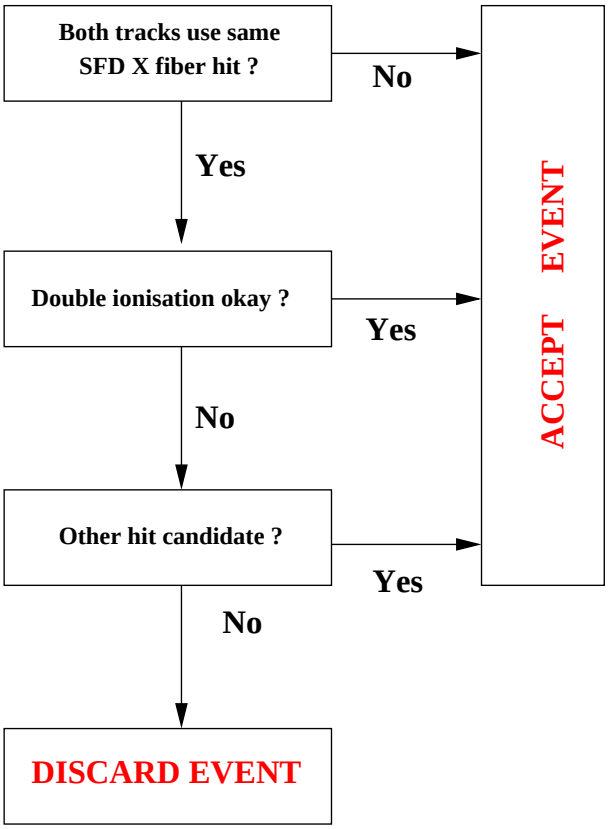

Figure 5: Decision tree for the track findinf at the level of SFD X.

entire column width.

4.5 Track finding in SFD Y

The track finding algorithm that we use for the SFD Y plane does not use the magnetic field description – which was used for the SFD X plane – but uses instead the track parameters as established in the DC system and the assumption that the tracks originate from the target. We developed this different algorithm in order to increase the accuracy of the SFD Y prediction. It is described in detail as an internal note [9].

Geometrical cut As for the SFD X plane, the geometrical cut used for the SFD Y plane includes a 3 σ intervall. The cut is defined as:

$$\text{Acceptance region} = 0.2 + \frac{4.8}{p_{tot}} \text{ cm} \tag{25}$$

For the timimg restriction, the algorithm controls the time difference between the VH and SFD Y as well as the time difference between the two SFD layers. The two cuts read:

Time cut VH - SFD Y In agreement with ARIANE the following cut is used:

$$\Delta t \text{ (VH} \rightarrow \text{SFD Y)} \leq \text{ Time of Flight } \pm 4 \text{ ns} \tag{26}$$

Time cut SFD X - SFD Y For the SFD Y time cut a 3 σ interval around the relative timing between the two planes of SFD is chosen. The relative timing is obtained by using single tracks and allowing only one hit per SFD plane. Figure

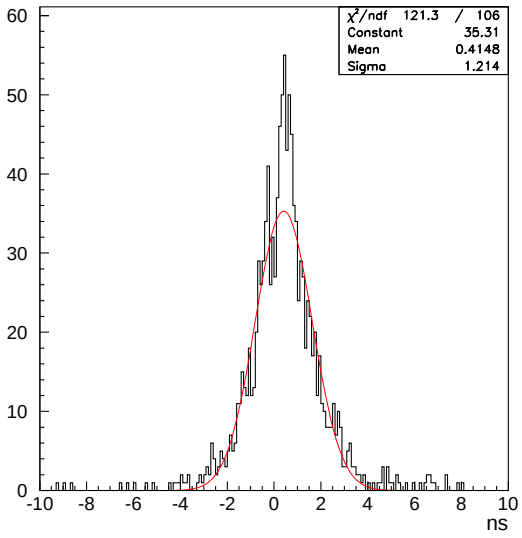

Figure 6: Time difference for single tracks between the two SFD planes. All events are required to have only one hit per SFD plane. The $\sigma_t \approx 1.2ns$, so a 3 σ environment would correspond to 3.6 ns. The mean equals 0.4 ns.

6 shows the relative timing of the two SFD planes. The mean is around 0.4 ns and the σ is around 1.2 ns, so we can take as a time cut for SFD Y:

$$\Delta t\text{(SFD X - SFD Y)} \leq 0.4 \pm 3 \cdot 1.2\ ns = 0.4 \pm 3.6\ ns \tag{27}$$

Double ionisation cut For events in which both tracks pass through the same SFD Y fiber, the program requires a time- and space correlated double ionisation signal in the Y layers of the DeDx. Figure 5 describes the decision tree also for the Y plane.

4.6 Smearing P_y within one fiber

As for the SFD X, the track program allows to distribute the track uniformly over the entire SFD Y slab width. This is achieved by randomly changing the measured y coordinate within one fiber. The Kalman filter procedure does then subsequently use the smeared value.

4.7 Track finding in the MSGC

The MSGC measurements are not used in the Baseltracking.

4.8 Target measurement

The target is included in the tracking as a measurement point. Specifically, the beam position is taken as the target's X and Y coordinate, the measured beam width then giving the uncertainty.

4.9 Upstream track fitting - Kalman filter procedure

After establishing the hit candidates in SFD X, the total momentum is fine-adjusted. Then the SFD Y hit candidates are found, as well as the target point and the Kalman filter routine is started to extrapolated the track parameters to the target.

Propagation of DC track parameters to SFD X First the DC track parameters and their covariance matrix are propagated through the magnet to SFD X. Then the covariance matrix is updated with all the MS coming from membranes in between.

State vector The state vector used for the Kalman filter can now be described as:

$$\hat{x}_t = \begin{pmatrix} x_{SFDX} \\ y_{SFDX} \\ z_{SFDX} \\ \frac{v_x}{v_z} \\ \frac{v_y}{v_z} \\ \frac{v_z}{v_z} = 1. \\ p_{tot} \end{pmatrix} \tag{28}$$

v_x, v_y and v_z are the x, y and z direction-vector of the track. v_x and v_y are normalised to v_z in the state vector (28). This normalisation has the convenient property that we can immediately calculate the momentum projections: Since the

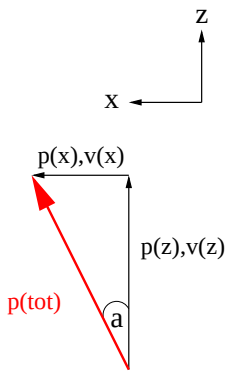

Figure 7: Geometry of the momentum. The red arrow symbolises the projection of the total momentum onto the XZ plane. The direction vectors and the momentum projections can be set into a correspondence $\frac{v_x}{v_z} = \tan(a) = \frac{p_x}{p_z}$.

normalisation of v_x with respect to v_z is directly tan(a), see figure (7), we have :

$$p_x^2 + p_y^2 + p_z^2 = p_{tot}^2 = ((\frac{v_x}{v_z})^2 + (\frac{v_y}{v_z})^2 + 1)\ p_z^2 \tag{29}$$

Hence knowing the total momentum and the direction vectors yields immediately the projections of the momentum on the x and y axis.

Kalman filtering The Kalman filtering now uses the SFD Y measurement and the target measurement to update the state vector and extrapolate it to the target. Figure (8) shows how Qy changes using the SFD Y measurement. Figure 9 il-

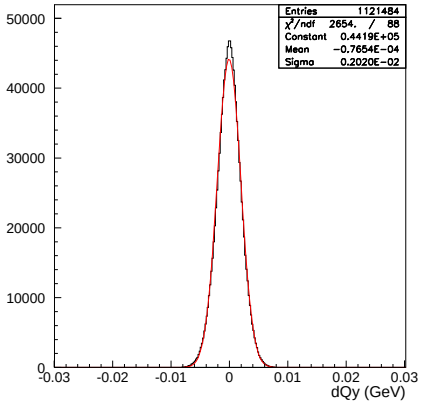

Figure 8: The change in Qy by applying the Kalman filter for the measurement obtained with the ARIANE method.

lustrates the target picture of reconstructed tracks before the target is put into the Kalman filter. It gives an idea of the accrued MS from the DC to the target.The x and y projections are shown in figure (10). Most tracks are within 1.5 cm in x direction and 2 cm in y direction.

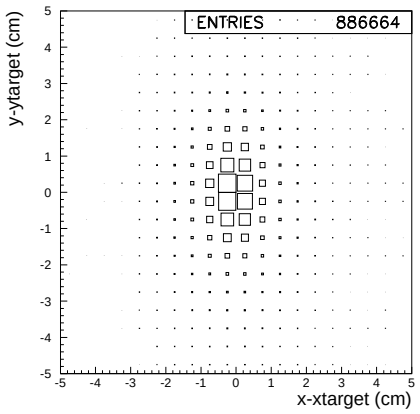

Figure 9: Target picture in the XY plane for tracks coming from arm 1.

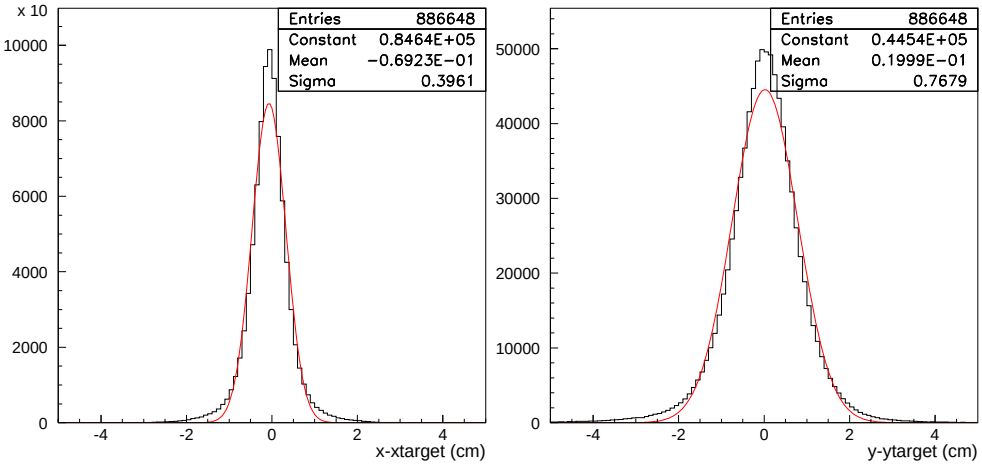

Figure 10: Target picture in the X or Y plane for tracks coming from arm 1.

The plots in figure 10 can be used to cross check the tracking algorithm: In x direction, the total momentum is corrected with a SFD X slab. This implies that the track passes through the SFD X slab and is very precisely defined at this point. The multiple scattering expected at the target in x direction comes therefore from

the way between the SFD X plane and the target. From MC we obtain that this corresponds to an uncertainty of:

$$\sigma_x = \frac{1.0}{p_{tot}} \text{ [GeV/c cm]} \tag{30}$$

On the other hand, the y direction of the track is precisely known at the first drift chamber. All uncertainty in the target in y direction comes therefore from the way between the first DC set and the target. Using MC we establish that this corresponds to an uncertainty of:

$$\sigma_y = \frac{2.0}{p_{tot}} \text{ [GeV/c cm]} \tag{31}$$

These values can now be used to cross check the track reconstruction: The mean of p_{tot} is around 2.5 GeV/c. Dividing the two MS values above by 2.5 yields

$$\sigma_x = \frac{1.0 \text{ [GeV/c cm]}}{2.5\text{[GeV/c]}} = 0.4 \text{ cm}$$

and

$$\sigma_y = \frac{2.0 \text{ [GeV/c cm]}}{2.5\text{[GeV/c]}} = 0.8 \text{ cm}$$

Comparing the thus obtained sigmas with the ones from the target projection in figure (10) shows that they are in good agreement.

4.10 Momentum calculation at the target

The state vectors of the tracks at the target level can be used to calculate the relative momenta in the CMS. We do this by first transforming the direction vector into the momentum projections, as demonstrated above in equation (29). Then the absolute momenta are transformed into the relative momenta by using a Lorenz transformation.

4.11 Overview of the BASEL tracking

An overview of the BASEL tracking is given in figure 11.

5 Treating accidentals like prompt events

As mentioned in section 4.1 the track finding for two track events at the SFD detector uses the timing in the vertical hodoscopes of both tracks. This method

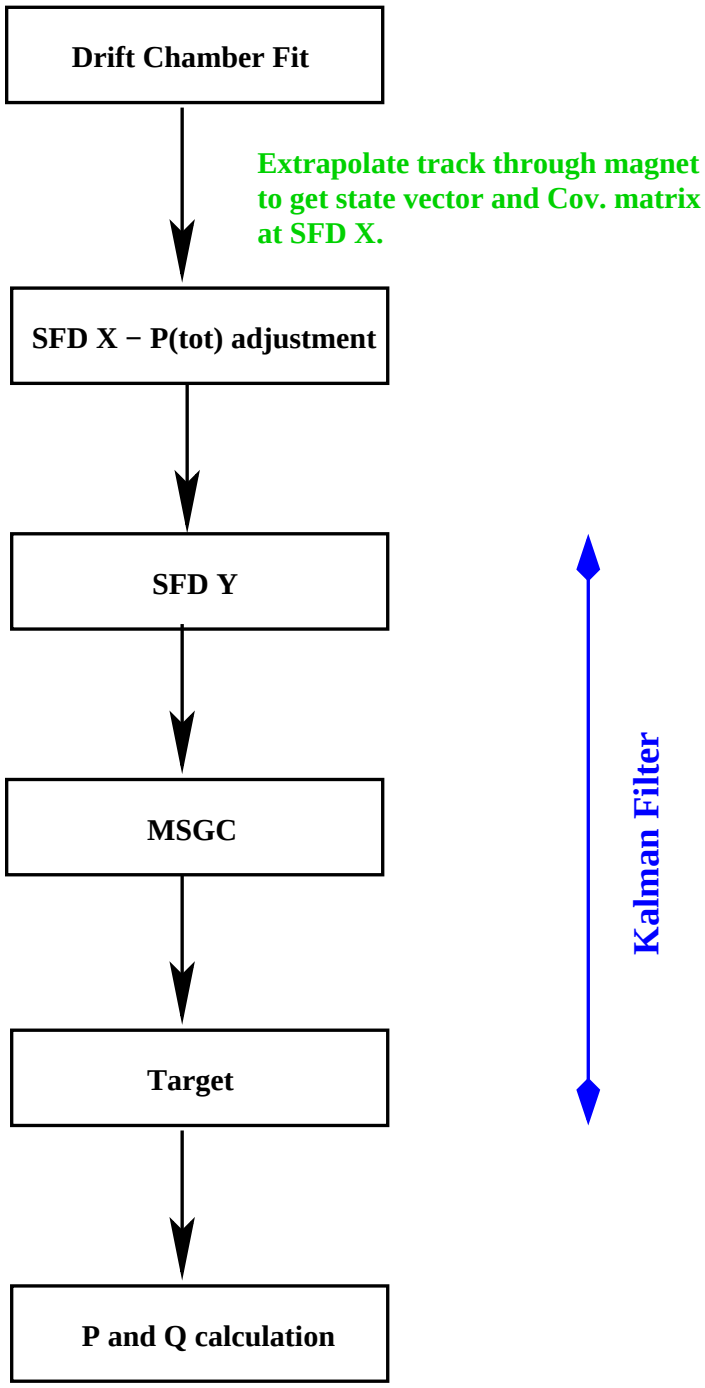

Figure 11: Flowchart of the BASEL tracking. The blue part corresponds to the part of the tracking where a Kalman filter was used.

treats prompt and accidental events equally; in both cases the use of two different time information creates an ambiguity for the track finding to select a hit fiber. This ambiguity would only exist for prompt events, but not for accidental events, if only the corresponding time of each track in the VH is used.

The use of the measured accidental spectrum for the analysis asks for a further correction to the accidentals: The peak-sensing circuit (PSC) [6] installed in the SFD detector treats accidental pairs and prompt pairs differently. If a time correlated event hits two adjacent fibers, they are sometimes merged into one single fiber. If, on the other hand, the absolute time difference between the two hits in the SFD is larger than 4 ns, the merging does not occur anymore. The inefficiencies of adjacent hit fibers due to the PSC was estimated previously [7, 8].

In addition, the read-out electronics of the SFD suppresses events which hit the same column in SFD, but are not time-correlated: The time gates of the TDC of the SFD are 20 ns. If an accidental event with a time difference in the VH of, say, 10 ns passes through the same fiber in the SFD X or Y layer, only one hit is recorded and the time stored being the earlier one. If the tracking then applies a time cut between the hit SFD fiber and the VH time, one track is rejected. Figure 12 illustrates the problem: Both tracks from an accidental pair event hit the same fiber at times t_1 and t_2, $t_1 < t_2$, but due to the open TDC gate of the SFD, only t_1 is recorded. If the tracking now requires a time cut between the VH and SFD X, i.e.

$$t_3 - t_1 < \text{tof (SFD} \rightarrow \text{VH)} \pm 3\sigma \tag{32}$$

then particle 1 will be reconstructed, since

$$t_3 - t_1 < \text{tof (SFD} \rightarrow \text{VH)} \pm 3\sigma \tag{33}$$

but particle 2 will not be reconstructed, because

$$t_4 - t_1 = t_4 - (t_2(th) - 10ns) = t_4 - t_2(th) + 10ns > \text{tof (SFD} \rightarrow \text{VH)} \pm 4ns \tag{34}$$

where $t_2(th)$ is the time where particle 2 would have hit SFD X. As a consequence, there are no accidental events reconstructed with adjacent hit fibers in the SFD as is displayed in figure 13. This situation can be remedied if the track finding algorithm uses not only the VH time of the track itself, say t_3 for track 1, but also the VH time of the other track, t_4. Since this procedure is included already to create an ambiguity for accidental events, no further corrections have to be applied.

The resulting SFD distributions for accidental and prompt events are displayed in figure 14. The Q of the plotted events was restricted to Q_{trans} <4 MeV/c and $|Q_l| < 15$ MeV/c.

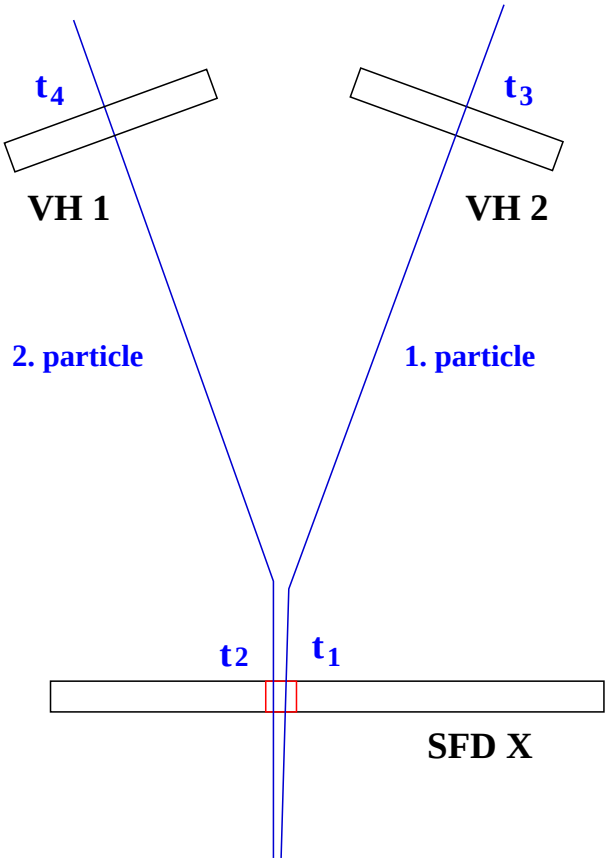

Figure 12: Time cut between VH and SFD in the BASEL tracking and its implication for accidentals.

6 Further improvements

In addition to the here presented tracking algorithm, the Basel tracking makes use of a new SFD Y determination method which has been described in detail previously [9].

7 Calibration and resolution

The behaviour of the here presented Basel tracking has been studied previously [10] using GEANT adapted to DIRAC [11] as a Monte Carlo program, and using the full detector and trigger simulation package [12] available. This section demonstrates the accuracy of the momentum determination using the Λ decay and it illustrates the resolution of the Q determination using Monte Carlo data.

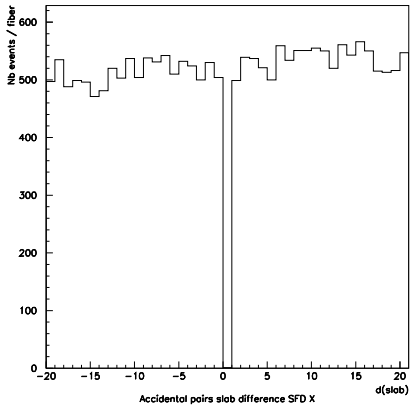

Figure 13: Difference of hit fibers chosen by the tracking for accidental pairs uncorrected.

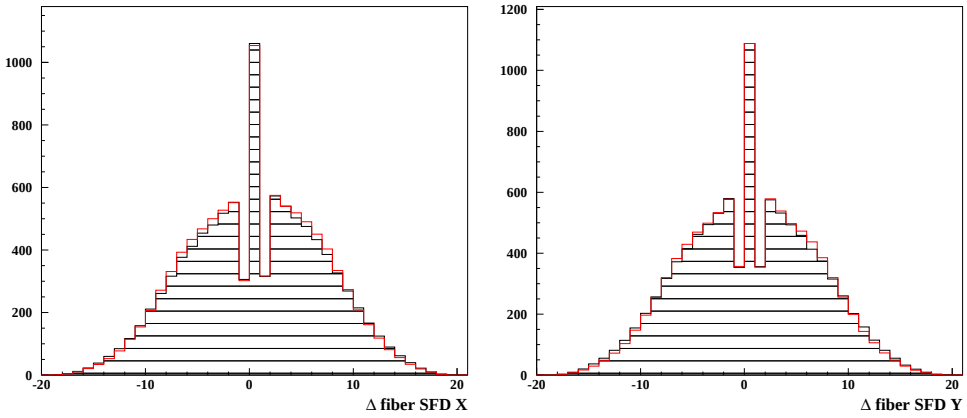

Figure 14: Difference of hit fibers chosen by the tracking for prompt (black) and accidental events (red) for Ni 2001 data in the X (left) and Y layer (right) of the SFD.

7.1 Accuracy of the momentum determination using Λ decays

The DIRAC spectrometer is able to capture some Λ's decaying into a proton and a negative pion:

$$\Lambda \rightarrow p + \pi^- \tag{35}$$

But due to the kinematics of this asymmetric decay, the symmetric DIRAC spectrometer can only capture events where the proton is reasonably fast. Hence a dedicated Λ trigger was implemented, which triggers only the outermost slab of the vertical hodoscopes on the positive arm, while accepting signals from all ver-

tical hodoscope slabs on the negative arm.

The reconstruction of the $p\pi^-$ invariant mass can be used to calibrate the spectrometer. For the nickel 2001 running period this was done and figure 15 shows the invariant mass of a proton and a negative pion pair. The total momentum was restricted to be 4.7 GeV/c $< p_\Lambda <$ 6.5 GeV/c. The red line represents a Gaussian

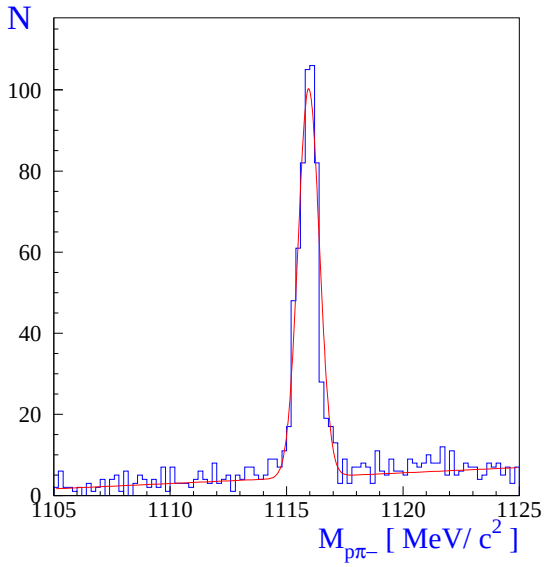

Figure 15: Mass distribution of $p\pi^-$ pairs from Λ decay at 4.7 $< p_\Lambda <$ 6.5 GeV/c
.

fit to the distribution with a mean value of 1115.6 MeV/c^2 and a width of σ_Λ=0.54 MeV/c in agreement with the PDG [13].

Figure 15 further establishes the resolution for Q. The Λ mass in the center of mass sytem is equal to

$$m_\Lambda^2 = (E_p + E_\pi)^2 = (\sqrt{m_p^2 + p^2} + \sqrt{m_\pi^2 + p^2})^2 \tag{36}$$

The relative monetum Q on the other hand can be written as:

$$Q^2 = (E_p - E_\pi)^2 - 4p^2 \tag{37}$$

Connecting the two equations and differentiating partially, one obtains:

$$dQ = \frac{m_\Lambda}{Q} \cdot dm_\Lambda \tag{38}$$

An estimated uncertainty in the Λ mass of σ_Λ=0.54 MeV/c, as shown in figure 15, translates therefore into an Q uncertainty of σ_Q=0.81 MeV/c.

7.2 Momentum resolution using Monte Carlo data

The difference between input and reconstructed laboratory momentum has been studied previously [10]. It amounts to dP_{tot} =7 MeV/c and $dP_x, dP_y = 1$MeV/c.

The relative momentum resolution has also been established previously [14] with Monte Carlo. Figure 7.2 established the relative momentum difference for dQ_x, dQ_y and dQ_l, which are defined as the difference between the input and the reconstructed value.

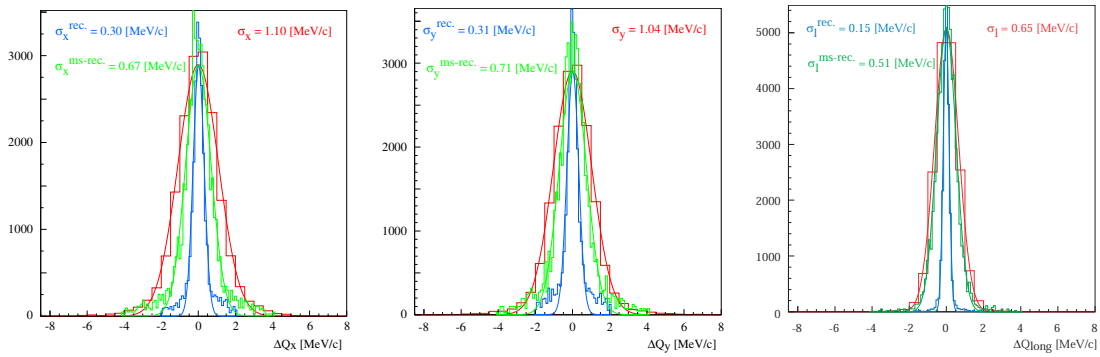

Figure 16: Difference between input and reconstructed value in relative momenta projections x, y and long (red). Shown for comparison the difference between the input value after the target and the reconstruction with full multiple scattering in the setup (green), as well as the difference between the input value after the target and the reconstruction without multiple scattering in the setup (blue).

The red curve indicates dQ_i taking into account the multiple scattering in the target and in the setup. The green curve compares the input Q after the target with the reconstructed one. The blue curve finally only consideres multiple scattering in the target, but not in the setup. Its resolution of 0.3 MeV/c for Q_x and Q_y and 0.15 MeV/c for Q_l gives therefore the resolution of the tracking algorithm without multiple scattering.

8 Conclusion

We developed an alternative tracking procedure which uses a different hit assignment algorithm. The calculation of the track parameters and their propagation has been done using a Kalman filter procedure upstream the magnet. The absolute and relative momentum determination is performed at the target level.

In addition, our tracking code treats accidental and prompt pair events equally by using for each track not only its intrinsic times, but also the times of the track

in the other arm. It further simulated the peak sensing circuit in the SFD detector also for accidental events and it allows two tracks from an accidental event to go through the same SFD fiber. These special treaments ensure that accidental pairs are reconstructed like prompt pair events. As a consequence, we are confident that the so reconstructed accidental spectrum is ideally suited for the main DIRAC analysis.

The absolute and relative momentum resolution has been established looking at Λ decays and using Monte Carlo data. The standard deviation of a Gauss fit to the Λ peak shows a reconstruction resolution of 0.54 MeV/c. The difference between input and reconstructed absolute and relative momenta is estimated to be dP_{tot} =7 MeV/c and $dP_x, dP_y = 1$MeV/c, dQ_x, dQ_y =1.1 MeV/c and dQ_l =0.65 MeV/c including the multiple scattering. The uncertainty in relative momentum only due to the tracking is established to be dQ_x, dQ_y =0.3 MeV/c and dQ_l =0.15 MeV/c, the difference to the former values being mostly the multiple scattering in the target.

References

[1] B. Adeva, et al. DIRAC: A high resolution spectrometer for pionium detection, NIM (2003).

[2] DIRAC analysis offline program ARIANE version 304-24.

[3] P. Maybeck, Stochastic Models, Estimation and Control, Volume 1. Academic Press, New York (1979).

[4] V. Yazkov, Description of the subroutine ClCovMtrDC.

[5] R. Fernow, Introduction to experimental particle physics, Paperback, Cambridge Univeristy Press (1989).

[6] A. Gorin, et. al. Peak-sensing discriminator for multichannel detectors with cross-talk. NIM A 452, 280-288 (2000).

[7] D. Goldin and L. Tauscher, Scintillating fiber detector efficiency study, DIRAC internal note 2003-02 (2003).

[8] F. Takeutchi, SFD Inefficiencies, Talk given at a DIRAC analysis meeting (2002).

[9] C. Schütz and L. Tauscher, The BASEL SFD Y prediction in the DIRAC experiment, DIRAC internal note 2002-04, (2002).

[10] C. Schütz and L. Tauscher, The behaviour of the BASEL extended tracking and the standard ARIANE tracking to $A_{2\pi}$ Monte Carlo data in the DIRAC experiment, DIRAC internal note 2002-01, (2002).

[11] GEANT version 3.21 adapted to the DIRAC experiment in its current version 2.61.

[12] Detector and trigger simulation package which is included in the current version of ARIANE 304-24.

[13] Particle data group (2002).

[14] A. Benelli, et. al., Systematic errors in the DIRAC experiment, DIRAC internal note 2003-01 (2003).